Progress In Electromagnetics Research C, Vol. 117, 203–219, 2021

Wideband Designs of Regular Shape Microstrip Antennas Using Modified Ground Plane

Venkata A. P. Chavali* and Amit A. Deshmukh

Abstract—Wideband designs of proximity fed regular shape microstrip antennas using bow-tie and H-shape ground plane profiles are proposed in the 1000 MHz frequency range. The modified ground plane alters the quality factor of the patch cavity which enhances the impedance bandwidth. In terms of the results obtained for the bandwidth and gain together, circular and square patches backed by bow-tie shape ground plane, followed by circular patch backed by H-shape ground plane yield optimum results. For substrate thickness of $0.097\lambda_g$, against the conventional ground plane, bow-tie shape gives 12% and 24% bandwidth increment for the circular and square patches, respectively, and H-shape ground plane yields bandwidth increment by 17% in the circular patch. All these wideband designs offer a peak gain around 6 dBi with a broadside radiation pattern. Further, a modified ground plane profile helps in optimizing the proximity fed antennas on lower substrate thicknesses. Amongst all the configurations, for $\sim 0.03\lambda_g$ reduction in the substrate thickness, square microstrip antenna using bow-tie shape ground plane yields 19% increase in the impedance bandwidth against the equivalent thicker substrate design with a peak broadside gain of above 6 dBi. Thus, the proposed modified ground plane antennas yield bandwidth improvement but for a smaller substrate thickness.

1. INTRODUCTION

The simplest method to enhance the bandwidth (BW) in microstrip antenna (MSA) is by employing a lower dielectric constant thicker substrate [1]. To negate the effect of higher probe inductance, proximity feeding has been employed to enhance the MSA BW for substrate thickness $> 0.07\lambda_g$ [2]. For substrate thicknesses in the range of $0.05\lambda_g - 0.07\lambda_g$, proximity feeding cannot be used as the capacitive nature of the impedance loci restricts the BW. An enhancement in the BW is achieved by using the concept of the multi-resonator technique. A simpler way of achieving this is the use of parasitic elements [1, 3–5]. With a single patch, MSA BW is increased by using slots or stubs [6–11]. However, these techniques are complex in design, and they require a thicker substrate to achieve optimum BW. Alternatively, defected ground plane structures (DGSs) have been used to increase the MSA BW [11–15]. Although a BW of more than 70% has been achieved here, the effects of modifications in the ground plane profile on the patch resonant modes and their impedances that yield wider BW have not been clearly explained.

In this paper, simpler novel wideband designs of regular shape MSA, i.e., circular MSA (CMSA) square MSA (SMSA), and equilateral triangular MSA (ETMSA), backed by bow-tie shape or H-shape ground plane profile are proposed in 1000 MHz frequency band. All the configurations have been studied in detail to explain the effects of modified ground plane profile on the BW enhancement. The modified ground plane alters the fringing field distribution in the cavity formed by the patch and the ground, and thus its quality factor that yields wider BW. Amongst all the designs, optimum results in terms of BW and gain are obtained in CMSA backed by bow-tie and H-shape ground plane and in SMSA backed by bow-tie shape ground plane. Against the conventional ground plane, BW increment by 12%

Received 2 November 2021, Accepted 22 December 2021, Scheduled 5 January 2022
* Corresponding author: Venkata A. P. Chavali (cpriyag14@gmail.com).
The authors are with the EXTC Department, SVKM's DJSCE, Mumbai, India.

and 24%, respectively in CMSA and SMSA by using bow-tie shape ground plane and by 17% in CMSA using H-shape ground, is achieved. In the two designs, a broadside peak gain of greater than 6 dBi is obtained. Further, the effects of employing a modified ground plane profile against the reduction in total substrate thickness, for the BW improvement, are studied. For the reduction in substrate thickness by 0.02–0.03λ_g, all the regular shape MSAs using modified ground plane achieve higher BW than that obtained with thicker substrate design using the proximity feed. Amongst all the designs, for $\sim 0.03\lambda_g$ reduction in total substrate thickness, SMSA using bow-tie shape ground plane yields 19% increase in the impedance BW against the equivalent thicker substrate design with a peak broadside gain of above 6 dBi. Thus modified ground plane design helps in realizing impedance matching to achieve larger BW using proximity feed but on smaller substrate thickness, where the conventional ground plane needs substrate thickness $\sim 0.1\lambda_g$. Thus the proposed study provides wideband designs of regular shape MSA on thicker and smaller substrate thickness offering more than 10–15% BW improvement. A detailed comparison highlighting the technical novelty in the proposed study is presented further in the paper. The proposed antennas are initially optimized using IE3D software [16], followed by the experimental validation using ZVH-8, FSC 6, and SMB 100 A. A reference wideband horn antenna was used in the radiation pattern and gain measurements. A three-antenna method is used to measure the gain.

2. REGULAR SHAPE MSAS USING BOW-TIE SHAPE GROUND PLANE

Proximity fed design of CMSA backed by bow-tie shape ground plane is shown in Figures 1(a), (b). The units of the patch dimensions and frequencies referred are in 'cm' and 'MHz', respectively. From the fabrication simplicity point of view for the modified ground, a three-layer suspended configuration is used, in which two layers of FR4 substrate ($\varepsilon_r = 4.3$, $h = 0.16$) are separated by an air gap of 'h_a' cm. Thus, on the total substrate thickness ($h_t = h_a + 2h$) of 2.62 cm ($\sim 0.09\lambda_g$), radius 'R' is parametrically

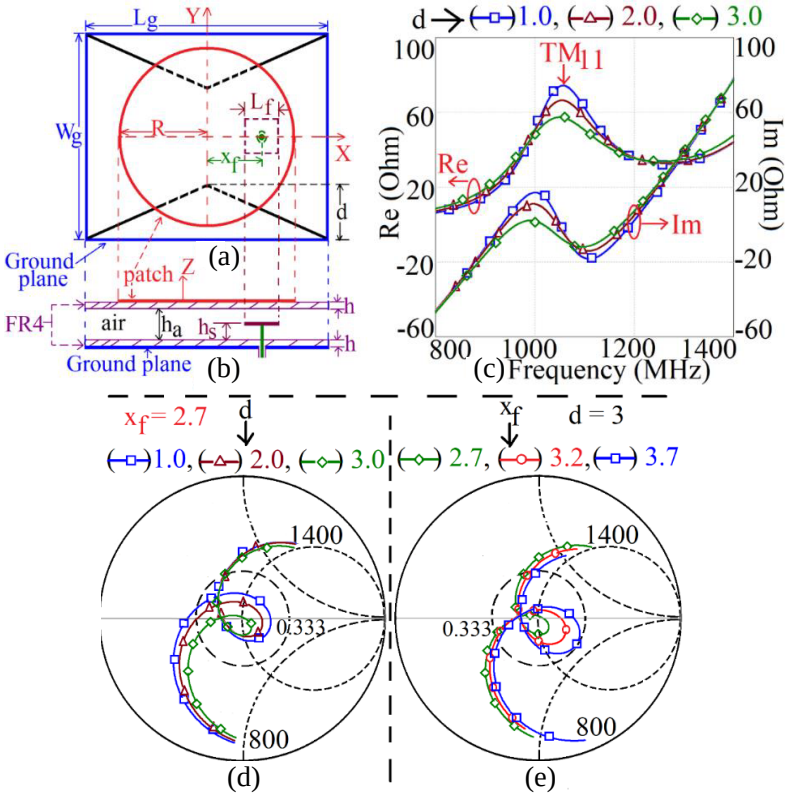

Figure 1. (a) (b) CMSA backed by bow-tie shape ground plane, and its (c) resonance curve plots, and smith chart for varying (d) 'd', and (e) 'x_f'.

optimized for $f_{\mathrm{TM11}} = 1050\,\mathrm{MHz}$. The radius is found to be 5.65 cm. To maintain a smaller profile of the antenna, a finite square ground plane of side length 'L_g' = 15 cm is selected. The proximity fed CMSA yields a simulated BW of 367 MHz (32.7%) with a peak broadside gain of 7.5 dBi. Further, a bow-tie shape ground plane profile is created by cutting a triangular notch of depth 'd' as shown in Figure 1(a). The slot to achieve the cross-polar reduction is placed along and below the patch edges. Against that triangular notch in the bow-tie shape is present inside and below the patch boundaries. This will alter the fringing field distribution thereby modifying the quality factor of the patch cavity at the fundamental mode. A detailed parametric study is carried out to analyze the effects of 'd', and the simulated resonance curve plots and Smith chart for the increment in 'd' for 'L_f' = 1.3, 'h_s' = 2.26, and 'x_f' = 2.7 cm are shown in Figures 1(c), (d).

With an increase in 'd', input impedance at TM_{11} mode decreases that reduces the corresponding loop size in the Smith chart. The decrease in the real part of the input impedance is attributed to the antenna cavity becoming lossy due to the detachment of the fringing fields from the bow-tie shape ground plane. At TM_{11} mode, the surface currents maxima are present in the patch center. As the triangular notch depth in bow-tie shape is not reaching the patch center, TM_{11} mode frequency remains constant. Since the modal current distributions are well discussed in the literature [1], they are not shown here for regular shape MSAs. Further, optimization of the feed position 'x_f' is carried out which increases the input impedance and thus the loop size in the smith chart to yield maximum BW, as shown in Figure 1(e). For $d = 3.0$, $x_f = 3.7$ cm, simulated and measured BWs of 468 MHz (42.12%) and 490 MHz (44.23%), respectively, are obtained, as shown in Figure 2(a). Across the BW, CMSA shows a peak broadside gain of 6.6 dBi. In comparison to the conventional ground plane, BW increment in the

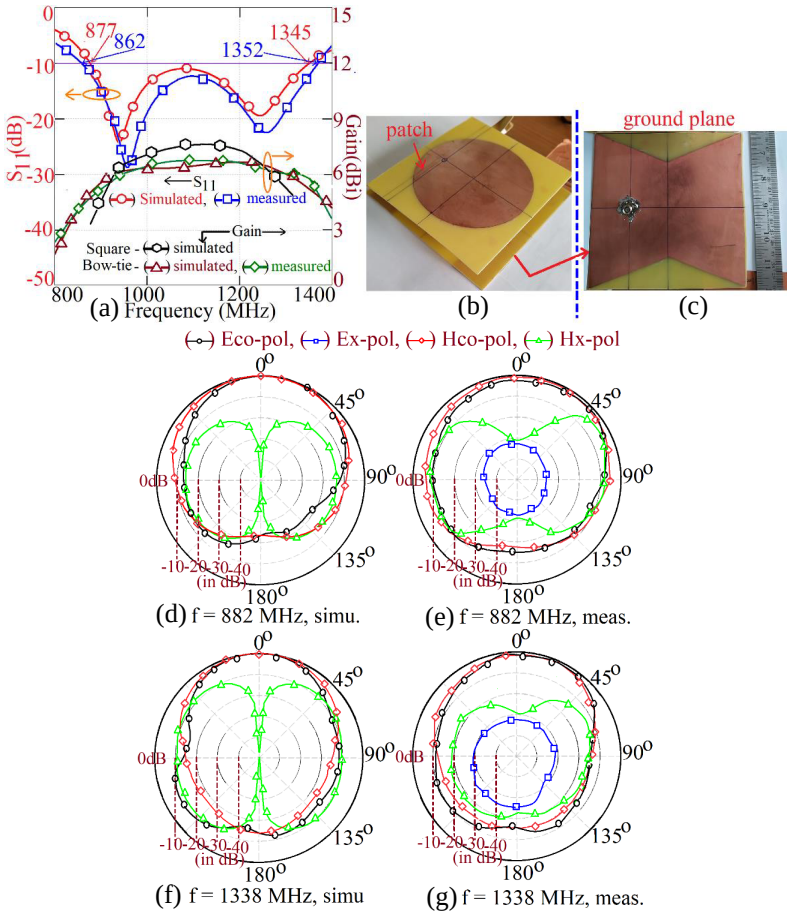

Figure 2. (a) Reflection coefficient (S_{11}) and gain plots, (b) (c) fabricated prototype, and radiation patterns nearer to the band, (d) (e) start, (f) (g) stop frequencies for CMSA backed by bow-tie shape ground plane.

measured result by above 11% is achieved. With a bow-tie shape ground plane, the cavity becomes lossy as more detachment of the fringing fields takes place. This reduces the quality factor of the antenna that increases the BW. Due to this, a small reduction in the antenna gain is noted. The fabricated antenna prototype is shown in Figures 2(b), (c). Radiation pattern plots near the band start and stop frequencies of the BW are shown in Figures 2(d)–(g).

Due to the presence of fundamental half wavelength mode on the patch over the complete BW, the radiation pattern remains in the broadside direction with E and H-planes aligned along $\Phi = 0°$ and 90°, respectively. Similarly, the designs of SMSA and ETMSA using bow-tie shape ground plane are optimized for the BW at their fundamental mode frequency. With reference to Figures 1(a), (b), SMSA or ETMSA is placed on the upper side of the top FR4 layer, with their orientation being symmetric to the ground plane from all the four sides. The SMSA length and ETMSA side length are selected to be '$2R$'. For this dimension, due to the respective patch geometries, fundamental mode frequency is different from 1050 MHz that changes the respective electrical substrate thickness value. Hence in each design, the air gap in the suspended configuration is adjusted such that the total substrate thickness is around $0.09\lambda_g$. Using a similar parametric study, SMSA and ETMSA designs are optimized for the BW, and the results for them are provided in Table 1 and shown in Figures 3(a), (b). An increment in the BW by nearly 24% in SMSA and 10% in ETMSA designs using bow-tie shape ground plane is achieved.

In both the designs, peak gain reduction by around 1 dBi is noted. The fabricated prototypes for SMSA and ETMSA designs are shown in Figures 3(c), (d) and 3(e), (f), respectively. For ETMSA backed by bow-tie shape ground plane, radiation pattern at the band edge frequencies as shown in Figures 4(a)–(d) and across the BW is in the broadside direction with cross-polar levels less than 15 dB as compared with the co-polar levels. The principle E and H-planes are aligned along $\Phi = 0°$ and 90°,

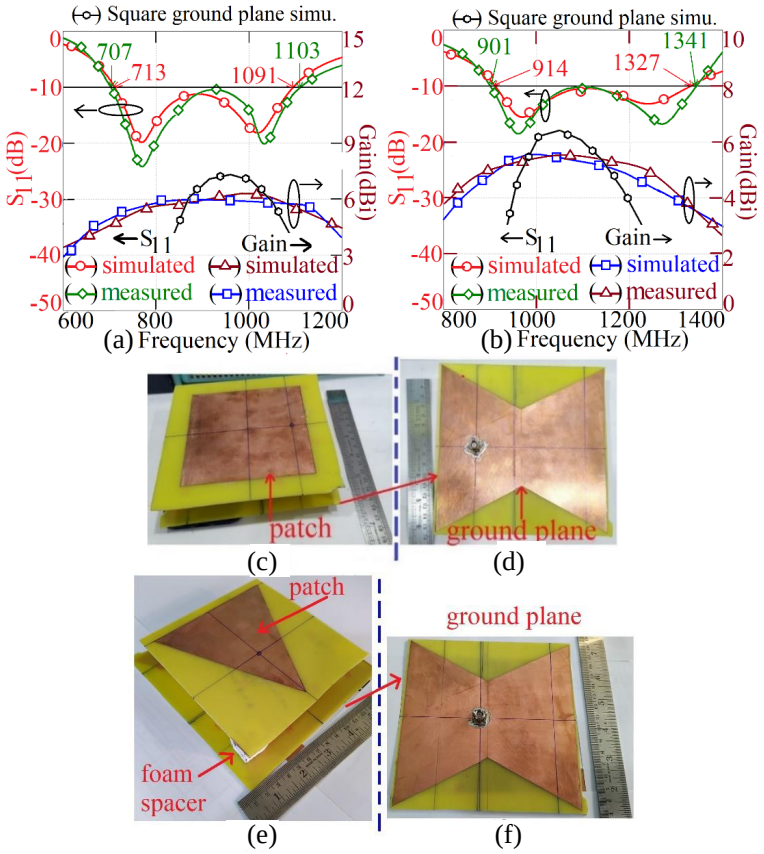

Figure 3. Optimum results for (a) SMSA, (b) ETMSA backed by bow-tie shape ground plane and fabricated prototypes of (c) (d) SMSA, (e) (f) ETMSA backed by bow-tie ground plane.

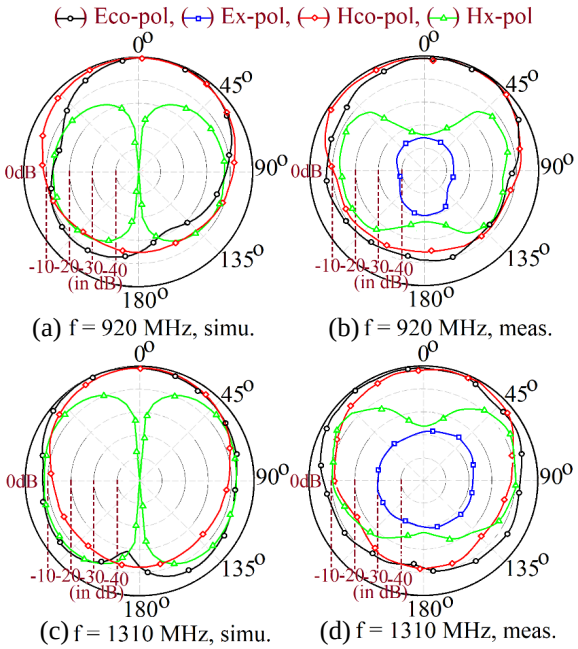

Figure 4. (a)–(d) Radiation pattern plots nearer to the band start and stop frequencies of the BW for ETMSA backed by bow-tie shape ground plane.

respectively. Similar radiation pattern characteristics are observed for the wideband SMSA backed by a bow-tie shape ground.

Although proximity feeding is the simplest method to increase the MSA BW, it cannot provide BW improvement for substrate thickness in the range of 0.05–0.07λ_g, or lesser. Therefore to study the effects of modified ground plane profile in proximity fed MSAs, a detailed study is carried out. The effects of air gap reduction in the suspended configuration are studied. Also, the effects of variation in triangular notch depth 'd' and proximity strip parameters are studied, and relevant plots for CMSA design are shown in Figures 5 & 6. With the reduction in air gap 'h_a', the impedance locus becomes capacitive in nature. This is due to the reduction in probe inductance with a reduced substrate thickness that makes the locus capacitive. The fundamental mode frequency increases, due to the reduction in fringing field extension with the substrate thickness that reduces effective patch radius. As shown in Figures 5(a), (b), for a reduction in 'h_a', with further increase in the feeding strip length 'L_f', the loop in the Smith chart can be optimized in the center. However, for this strip length variation, it was observed that the loop position cannot be fully optimized inside VSWR = 2 circle for the maximum BW. Hence, the effects of the increase in 'd' (bow-tie ground parameter) are studied. With an increase in 'd', the cavity becomes lossy reducing the input impedance in the resonance curve and the loop size in the Smith chart. To optimize this loop position inside VSWR = 2 circle as shown in Figures 5(e), (f), feed strip length 'L_f' is increased. This parametric process yields the optimal position of the loop size inside VSWR = 2 circle. To achieve the maximum BW, the impedance at TM_{11} mode is increased by increasing 'x_f' which leads to a larger loop size and thus the optimum BW. Through this parametric process, CMSA backed by a bow-tie shape ground plane is optimized for the BW on reduced substrate thickness. Various antenna parameters in the optimum design are given in Table 1. The simulated and measured BWs are 436 MHz (38.8%) and 469 MHz (41.1%), respectively with a peak broadside gain of 6.1 dBi, as shown in Figure 6(c). The pattern characteristics for this design are similar to its thicker substrate variation. Thus against the CMSA design on the thicker substrate (0.097λ_g), the design using smaller substrate thickness (0.069λ_g) yields 8.4% increase in the BW with a smaller reduction in the broadside gain. The improvement in the BW is attributed to the lossy antenna cavity which is due to the bow-tie shape ground plane profile. Using a similar parametric process, designs of SMSA and ETMSA backed by bow-tie shape ground plane are optimized on smaller substrate thickness, and their results are tabulated in Table 1.

Table 1. Results for optimum regular shape MSAs using Bow-tie shape ground plane (R: CMSA radius, L: SMSA length, S: ETMSA side Length, λ_g: wavelength resonant mode frequency).

MSA + ground plane profile	h_t, h_s	L_g	$R/L/S$	d, l_g	L_f, x_f	Meas. BW, (MHz, %)	% increment in BW	Gain dBi	f_{11}/f_{10}	ε_{re}	h_t/λ_g
CMSA + Square	2.62, 2.26	15	5.65	0, –	1.4, 2.7	367, 32.7	–	7.5	1055	1.103	0.097
CMSA + Bow-tie	2.62, 2.26	15	5.65	3, –	1.4, 3.7	490, 44.23	11.53	6.6	1032	1.103	0.094
CMSA + Bow-tie	1.82, 1.46	15	5.65	4, –	1.9, 4.0	469, 41.1	8.4	6.1	1061	1.156	0.069
SMSA + Square	2.92, 2.56	15	11.3	0, –	1.5, 2.7	190, 19.89	–	6.9	926	1.091	0.0941
SMSA + bow-tie	2.92, 2.56	15	11.3	4, –	1.7, 4.2	396, 43.75	23.86	6.2	867	1.091	0.9
SMSA + bow-tie	2.02, 1.66	15	11.3	4.5, –	2.2, 4.5	351, 39.1	19.21	6	885	1.138	0.0635
ETMSA + Square	2.62, 2.26	15	11.3	0, –	1.2, 6	359, 29.4	–	6.4	1140	1.103	0.104
ETMSA + bow-tie	2.62, 2.26	15	11.3	4.0, –	1.8, 6.6	440, 39.25	9.85	5.4	1002	1.103	0.091
ETMSA + bow-tie	2.2, 2.2	15	11.3	4.5, –	1.5, 0.9	473, 37.14	7.74	5.4	1170	1.138	0.084

Using SMSA with bow-tie shape ground plane, the reduction in substrate thickness by $0.03\lambda_g$ is achieved, which yields simulated and measured BWs of 325 MHz (36.29%) and 351 MHz (39.1%), respectively, with a peak broadside gain of 6 dBi. Thus for the reduction in peak gain by nearly 1 dBi, the bow-tie ground plane on a smaller substrate yields more than 16% BW increment. In ETMSA, for the optimum result using the bow-tie shape ground plane, a reduction in the substrate thickness by $0.02\lambda_g$ is observed. Here, the simulated and measured BWs are 439 MHz (34.5%) and 473 MHz (37.14%) respectively with a peak broadside gain of 5.4 dBi. Against the design on substrate thickness of $0.1\lambda_g$, an increase in the BW by 7.7% is noted. However, the gain reduction in ETMSA is more. This is attributed to the asymmetrical nature of the resonant fields at the fundamental mode in ETMSA against that in CMSA and SMSA, on the bow-tie shape ground plane profile. Thus, across all the regular shape MSAs using proximity feed, the bow-tie shape ground plane yields reduction in substrate thickness by 0.02–$0.03\lambda_g$ and shows BW improvement by around 10%. To avoid the repetition of the data, fabricated prototype images of the antennas and radiation pattern plots for every optimum design on reduced substrate thickness are not shown. In each design discussed above, using parametric optimization, an optimum case is considered where the maximum possible values of the BW and gain together are achieved. Based on these criteria, optimum results are presented in Table 1 for the bow-tie ground plane as well as in the H-shape ground plane profile configurations as discussed in the following section.

3. REGULAR SHAPE MSAS USING H-SHAPE GROUND PLANE

Proximity fed designs of CMSA, SMSA, and ETMSA backed by H-shape ground plane using a three-layer suspended configuration are shown in Figures 7(a)–(c). In this ground plane profile, slot length 'l_g' and width 'd' are present below the patch that will modify the fringing field distribution in the patch

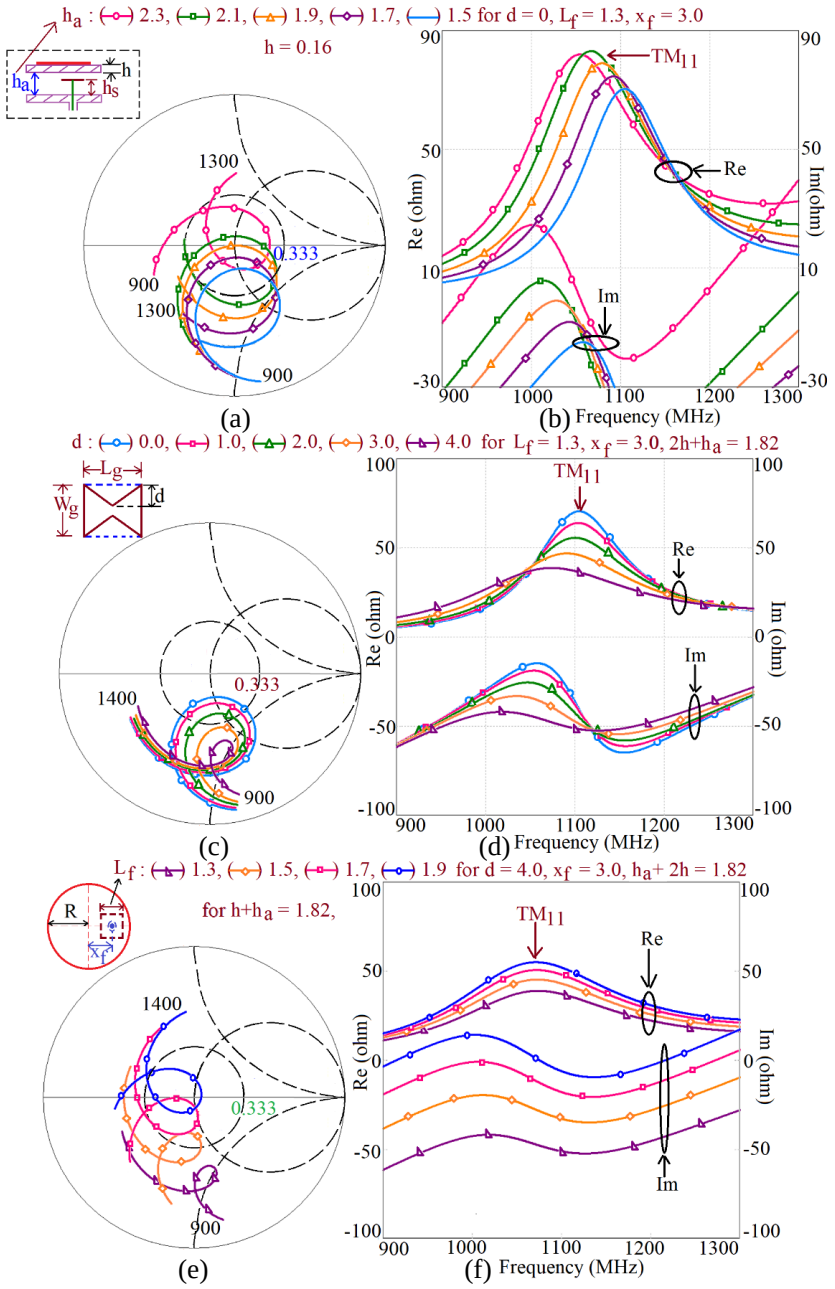

Figure 5. Smith charts and resonance curve plots for variation in (a) (b) h_a, (c) (d) d and (e) (f) L_f for proximity fed CMSA backed by finite bow-tie shape ground plane.

cavity. Therefore, the effects of variation in these parameters are investigated for the BW improvement.

Against the variation in slot parameters, resonance curve plots and surface current distribution were studied. In this ground plane profile similar effects in the patch parameters are also observed, which are noted in the bow-tie design. Both 'l_g' and 'd' affect the impedance BW. But the length 'l_g' has more effects since it leads to a larger slot area on the ground plane below the patch that reduces the patch quality factor thereby realizing more detachment of the fringing fields to yield BW increment. In each design, BW optimization is realized by varying 'l_g', 'd', and 'x_f', and the results for the CMSA variation are shown in Figure 8(a). In CMSA, for 'd' = 3, 'l_g' = 8, and 'x_f' = 4.3 cm, simulated and measured BWs of 518 MHz (46.29%) and 556 MHz (49.6%), respectively, are obtained. The antenna shows a peak broadside gain of greater than 6 dBi. As compared with the conventional ground plane,

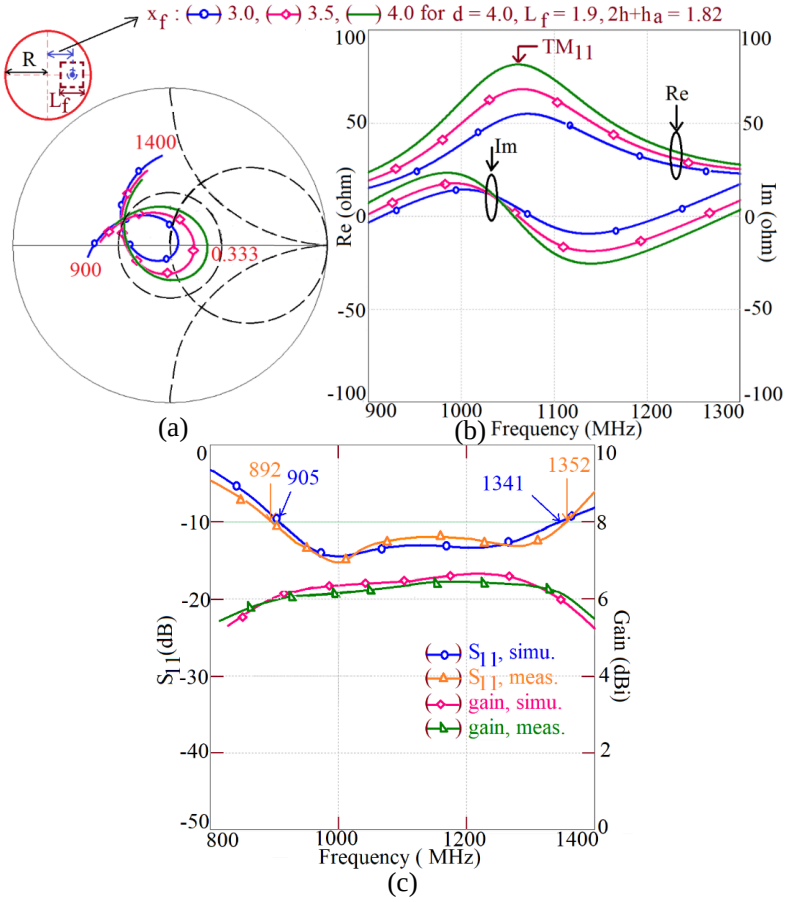

Figure 6. (a) (b) Smith chart and resonance curve plots for the variation in feed point location, and (c) optimum results for CMSA backed by bow-tie shape ground plane on smaller substrate thickness.

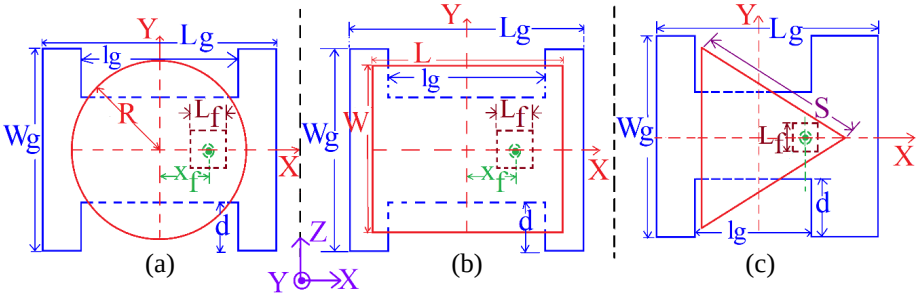

Figure 7. (a) CMSA, (b) SMSA, and (c) ETMSA backed by H-shape ground plane.

17% increment in the BW but with 1.3 dBi decrement in the peak broadside gain is observed. The fabricated antenna is shown in Figures 8(b), (c).

Using the H-shape ground plane, radiation pattern plots for CMSA near the band start and stop frequencies are shown in Figures 8(d)–(g). Due to the fundamental TM_{11} mode currents on the patch, a broadside radiation pattern is observed over the complete BW with a cross-polar level less than 15 dB as compared with the co-polar component. Using a similar study, the design of SMSA with an H-shape ground plane is optimized for the BW, and results for them are summarized in Table 2. Against the conventional ground plane, an increase in the BW by 14% is obtained. The antenna yields a broadside radiation pattern over the BW with a peak gain above 5.5 dBi. In the ETMSA design using the H-shape

Table 2. Results for optimum regular shape MSAs using H-shape shape ground plane (R: CMSA radius, L: SMSA length, S: ETMSA side Length, λ_g: wavelength resonant mode frequency).

MSA + ground plane profile	h_t, h_s	L_g	$R/L/S$	d, l_g	L_f, x_f	Meas. BW, (MHz, %)	% Increment in BW	Gain dBi	f_{11} or f_{10}	ε_{re}	h_t/λ_g
CMSA + Square	2.62, 2.26	15	5.65	0, –	1.4, 2.7	367, 32.7	–	7.5	1055	1.103	0.097
CMSA + H-shape	2.62, 2.2	15	5.65	3, 8	1.4, 4.3	556, 49.6	16.9	6.2	1038	1.103	0.095
CMSA+ H-shape	1.82, 1.46	15	5.65	3, 8	1.7, 4.3	627, 52.2	19.5	5.5	1082	1.156	0.0705
SMSA + Square	2.92, 2.56	15	11.3	0, –	1.5, 2.7	190, 19.89	–	6.9	926	1.091	0.0941
SMSA + H-shape	2.72, 2.36	15	11.3	4, 8	1.5, 4.3	329, 34	14.11	5.7	876	1.099	0.083
SMSA + H-shape	2.02, 1.66	15	11.3	4, 8	2.2, 4.6	352, 39	19.11	5	894	1.138	0.0642
ETMSA + Square	2.62, 2.26	15	11.3	0, –	1.2, 6	359, 29.4	–	6.4	1140	1.103	0.104
ETMSA + H-shape	2.62, 2.26	15	11.3	3.5, 3	1.5, 1.8	412, 38.11	8.71	4.9	1162	1.103	0.1065
ETMSA + H-shape	1.02, 1.66	15	11.3	4.0, 8	1.6, 0.9	504, 39.5	10.1	4.7	1170	1.138	0.0841

ground plane, BW increment by 9% is achieved, but the peak gain is reduced below 5 dBi. The reduction in gain in ETMSA design is attributed to the asymmetrical nature of the patch geometry against the H-shape ground plane.

The effects of substrate thickness reduction in the proximity fed MSAs using the H-shape ground plane profile are studied here. The Smith chart and resonance curve plots highlighting the parametric study for the variation in 'h_a', 'd', 'L_f', and 'x_f' for CMSA backed by H-shape ground plane are shown in Figures 9 & 10. With the reduction in 'h_a', which reduces the total substrate thickness, the impedance locus in the Smith chart becomes capacitive in nature. Further for any value of the strip length 'L_f', the loop for reduced substrate thickness cannot be optimized completely inside VSWR = 2 circle. An increase in 'd' for lower substrate thickness reduces the impedance at the resonant mode, which further reduces the loop size. The loop position and its size are further optimized for maximum BW by changing the strip length and position 'x_f'. This parametric process yields optimum BW, and the results for CMSA design are shown in Figure 10(c). Antenna dimensions for the CMSA backed by H-shape ground plane on reduced substrate thickness are $h_t = 2.02$, $d = 3.0$, $R = 5.65$, $L_f = 1.7$, $x_f = 4.3$ cm, and its simulated and measured BWs are 593 MHz (48.6%) and 627 MHz (52.2%), respectively. The antenna shows a peak broadside gain of 5.5 dBi. Using similar parametric optimization, SMSA and ETMSA backed by the H-shape ground plane are optimized on reduced substrate thickness. The optimum dimensions and results for the CMSA, SMSA, and ETMSA with the H-shape ground plane are provided in Table 2.

The SMSA backed by H-shape ground plane on a lower substrate thickness of $0.0642\lambda_g$ yields a simulated BW of 325 MHz (36.29%) whereas the measured BW is 352 MHz (39%), offering peak broadside gain of 5 dBi. Similarly, ETMSA on H-shape shape ground plane realizes simulated and measured BWs of 461 MHz (361%) and 504 MHz (39.5%), respectively, with a peak gain of 4.7 dBi along the broadside direction. In all the regular shape MSA variations on smaller substrate thickness

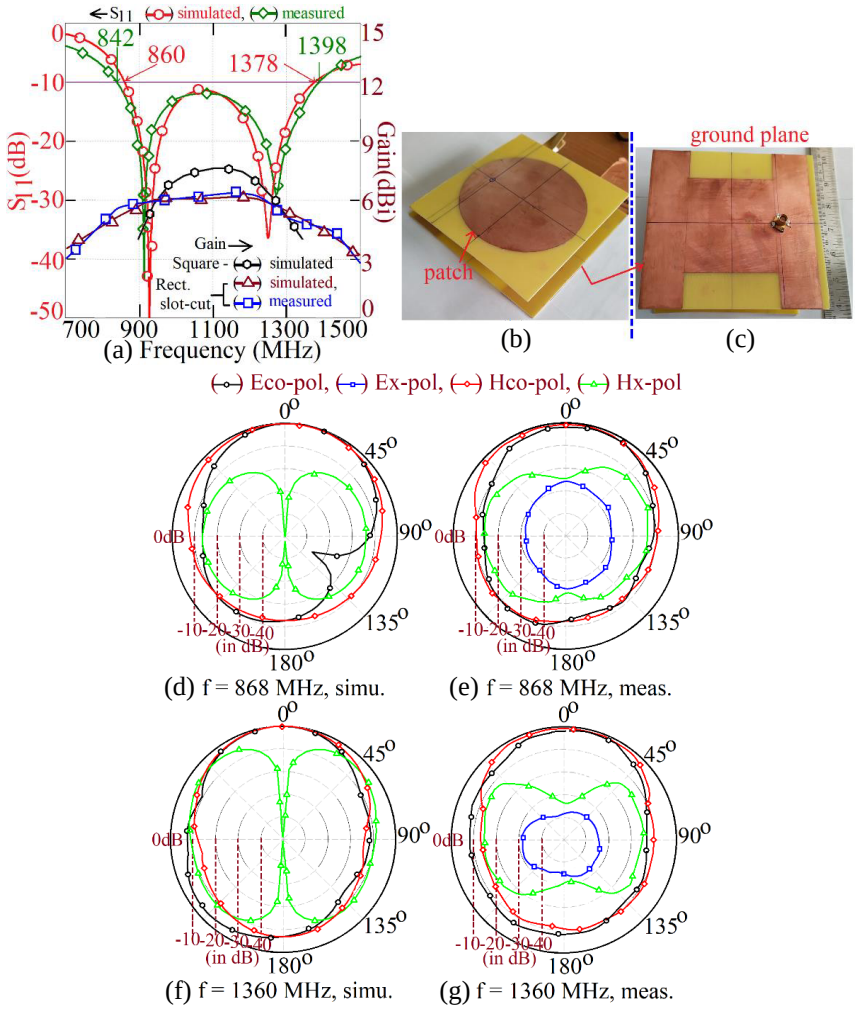

Figure 8. (a) Optimum results, (b) (c) fabricated prototype, (d)–(g) radiation pattern plots near the band start and stop frequencies of the BW for CMSA backed by H-shape ground plane.

0.02–$0.03\lambda_g$, the reduction in thickness is obtained with more than 10% BW increment. Here amongst all the designs, SMSA backed by a bow-tie shape ground plane offers optimum results in terms of BW and gain together for $\sim 0.03\lambda_g$ (i.e., for a reduction in total substrate thickness). In all the above designs using bow-tie and H-shape ground planes, BW increment is attributed to the reduction in the quality factor of antenna cavity, which also accounts for smaller gain reduction. Further optimum results in terms of BW increment against smaller reduction in gain in thicker and smaller substrate thickness are obtained in CMSA and SMSA designs. This is attributed to the symmetry in resonant field distribution at the fundamental mode against the modified ground plane. This symmetry is not present in ETMSA, and thus it does not offer optimum results in terms of BW, gain for thicker and smaller substrate, using the proximity feed.

Another important parameter in the wideband design using a modified ground plane is the back lobe radiation level with reference to the front lobe and the crosspolar level variation over a wide angular range as against the conventional ground plane design. For all the MSAs proposed on the total substrate thickness of 0.09–$0.1\lambda_g$, simulated plots of the front to back lobe (F/B) radiation level against the frequencies are shown in Figure 11. Here, the level at 0° represents the front lobe level, and that at 180° represents the back lobe level. Also the radiation pattern plots for the regular shape MSAs against different ground plane profiles are shown in Figure 12. In all the designs, MSA with a bow-tie shape ground plane offers improved F/B performance, thereby exhibiting lower back lobe

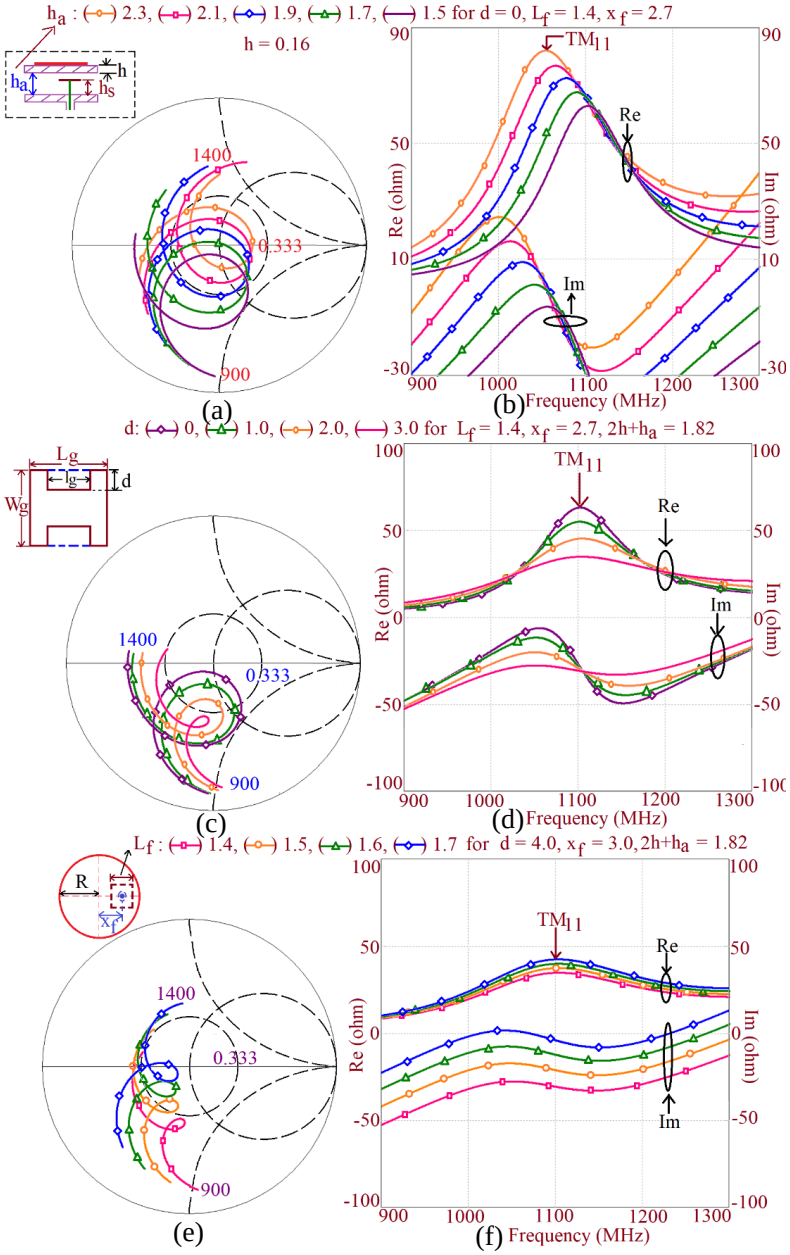

Figure 9. Smith charts and resonance curve plots for the variation of (a) (b) substrate thickness, (b) (c) ground plane depth 'd', (e) (f) feed strip length 'L_f' of CMSA with H-shape ground plane.

radiation. In SMSA design, the maximum difference between the front lobe and back lobe levels is noted over the complete BW. In MSA using a finite ground plane, the back lobe radiation is attributed to the diffraction of the electromagnetic energy from the edges of the ground plane as well as due to the excitation of surface waves [23–27]. The bow-tie shape ground plane profile minimizes the diffraction and surface wave excitation effects and thus focuses the energy in the forward direction. This gives lower back lobe radiation level and thus an improved value of the F/B ratio. The optimum result for the F/B ratio in SMSA is attributed to the uni-directional current variation over the patch and most of the ground plane area, due to the exciting TM_{10} mode. The extent of uni-directional modal current nature decreases in CMSA and further in ETMSA designs. Another factor that adds to the back lobe radiation is the common mode current excitation [29, 30]. The common mode current arises due to the

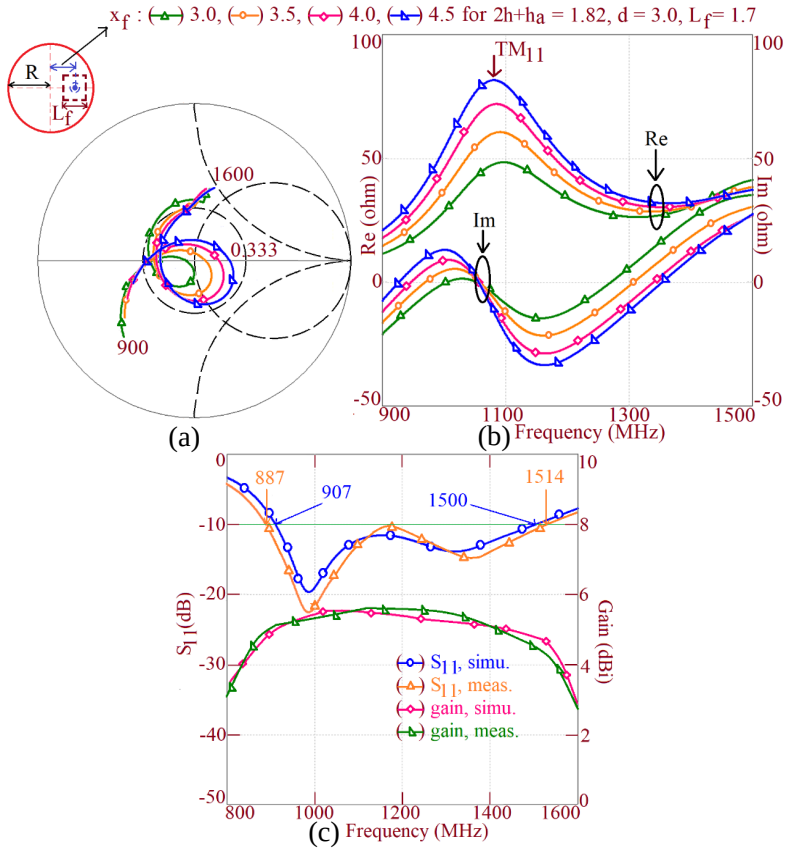

Figure 10. (a) (b) Smith charts and resonance curve plots for the variation in feed point location, and (c) S_{11} and gain plots for the CMSA backed by H-shape ground plane for $h_t = 1.82\,\text{cm}$.

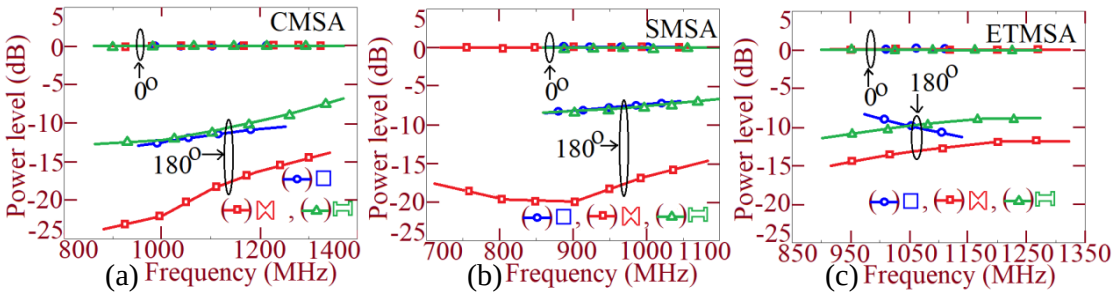

Figure 11. Simulated Eco-polar plots at 0° and 180° against frequency for (a) CMSA, (b) SMSA, and (c) ETMSA with different ground plane profiles.

imperfections in the antenna design with respect to the feed. The bow-tie shape ground plane profile offers less discontinuities in the structure as against the H-shape ground and thus offers less back lobe radiation and better F/B ratio.

The geometry of the H-shape ground plane is similar to that of a conventional square ground plane, except near the vertical dimensions of the H-shape slot. Also, these vertical edges of the slot are not present near the maximum impedance region on the ground plane at the fundamental mode. Due to these differences in the geometrical aspect against the bow-tie shape, the H-shape ground plane does not provide suppression of the surface waves and reduced diffraction effects from the ground plane edges. Hence, the back lobe radiation observed is higher than or the same as that of the conventional ground

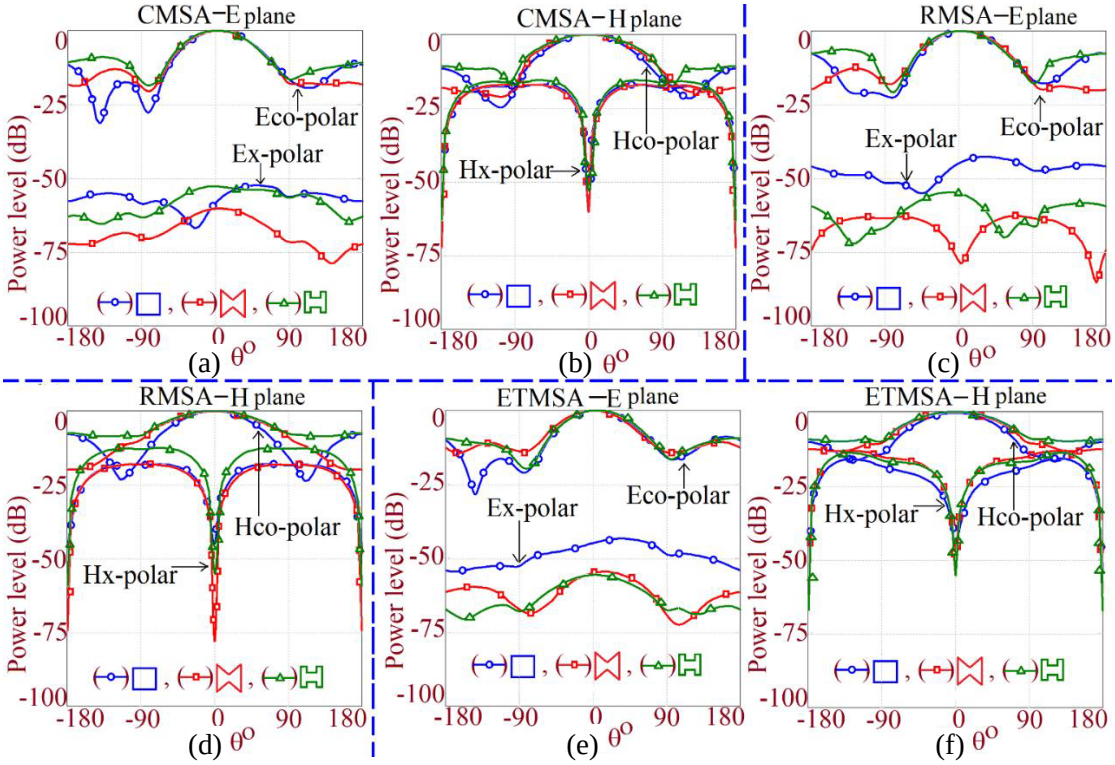

Figure 12. Simulated radiation pattern plots at center frequency of BW for (a) (b) CMSA, (c) (d) SMSA, (e) (f) ETMSA with modified ground plane profiles.

plane. In all the initial designs of regular shape MSAs backed by bow-tie shape ground plane, with respect to the fundamental mode frequency, the substrate thickness is selected in the range of 0.09–0.1λ_g. Towards higher frequencies of the BW in those designs the electrical substrate thickness exceeds 0.1λ_g. The increased substrate thickness supports the excitation of surface waves which increases the back lobe radiation towards those frequencies. Further, in all the designs, the bow-tie shape ground plane offers lower cross-polar levels, specifically in the E-plane of radiation. Here, amongst all the designs, SMSA using a bow-tie shape ground plane shows the lowest cross-polar level over a wider angular range. The lower cross-polar radiation is attributed to the increase in the second-order orthogonal mode frequency of the patch, which is the primary source of cross-polar radiation at the fundamental mode. However, the similar cross-polar reduction is not observed in the H-plane. This difference in the cross-polar levels in the two planes is attributed to the use of an electrically thicker substrate. Hence, the proposed work does not claim to present a lower cross-polar design, but only a wideband design employing simpler ground plane modifications.

In all the proposed modified ground plane designs, BW increment is achieved at the cost of a slight reduction in the broadside gain. In every parametric iteration discussed above, for each of the configurations, an optimum design is selected where a smaller reduction in the broadside gain against a substantial increase in the BW is achieved. Thus, the optimum configuration is considered when the gain and BW together are optimum for the given substrate thickness. Thus, for substrate thickness in the range of 0.09–0.1λ_g, designs of CMSA and SMSA using bow-tie shape ground plane yield optimum performance in terms of the BW with a smaller reduction in the broadside peak gain. Using the H-shape ground plane, amongst all the MSA variations, CMSA yields optimum results. On smaller substrate thickness, amongst all configurations, SMSA design backed by bow-tie shape yields substantial increment in BW against thicker substrate design using the conventional ground plane, with a peak gain of 6 dBi. To highlight the technical novelty in the proposed work, these wideband designs are compared against some of the reported wideband designs as given in Table 3. The patch area (A) and substrate thickness as mentioned in Table 3 are normalized with respect to the wavelength 'λ_c' at the center frequency of

Table 3. Comparison of optimum designs against reported wideband antennas.

Antenna shown in	Broadband technique used	Meas. BW (%)	Gain (dBi)	h_t/λ_c	A/λ_c (cm)
CMSA + bow-tie H = 2.62	bow-tie ground plane	44.23	6.6	0.101	3.83
SMSA + bow-tie H = 292	bow-tie ground plane	43.75	6.2	0.9	4.02
SMSA + bow-tie, $h = 2.2$	bow-tie ground plane	39.1	6.0	0.0645	4.077
CMSA + H-shape, $h = 262$	H-shape ground plane	49.6	6.2	0.102	3.93
Ref. [3]	Gap coupled	38.4	7.21	0.1129	3.897
Ref. [4]	Gap coupled	6.8	7	0.04	0.741
Ref. [5]	Gap coupled	20.1	9.5	0.053	6.137
Ref. [6]	Slot-cut	68	10	0.02	2.244
Ref. [7]	Slot-cut	44	9.9	0.09	5.975
Ref. [8]	Slot-cut	CMSA-13.45	13.7	0.046	8.35
		RMSA-12.4	14	0.047	9.213
Ref. [9]	Slot-cut	21.49	8.5	0.1	1.5
Ref. [10]	Slot-cut	24	–	0.041	6.82
Ref. [11]	Stub loaded	14.5	10	0.054	2.787
Ref. [12]	DGS	86.79	4.1	0.065	1.223
Ref. [13]	DGS	141	6.2	0.055	1.15
Ref. [14]	DGS	103	4.35	0.046	0.578
Ref. [15]	DGS	72.87	–	0.068	1.673
Ref. [18]	DGS	12.88	1.8	0.014	–
Ref. [19]	DGS	13.05	9.76	0.056	0.66
Ref. [20]	DGS	12.2	8.7	0.108	1.344
Ref. [21]	DGS	12	8.9	0.02	3.6
Ref. [22]	DGS	28.8	8	0.08	3
Ref. [28]	Resonant cell loaded	9	7	0.04	5.4

the BW. Hence, the values of 'h_t/λ_c' will differ from those mentioned in Tables 1 & 2.

The gap coupled configurations in [3–5] realize larger gain than the proposed configurations, but the BW obtained is smaller though the design includes multiple resonant modes. Larger BW on a substrate which is thinner than the proposed CMSA and SMSA is backed by modified ground plane profile. But it employs differential feeding and shows conical radiation patterns due to the presence of higher order modes. A larger gain reported in [7, 8] is due to the higher patch size whereas the MSA reported in [9] does not offer wider BW around the fundamental patch mode. The sectoral MSA designs reported in [10, 11] require additional shorting post, slot, or stub, and yet offer smaller BW. Although the designs reported in [12–15] offer substantially higher BW, the reported configurations are complex in design, and they do not provide explanations for the antenna functioning in terms of the patch resonant modes. In comparison, the proposed designs are simpler in implementation, since it just requires a modified

ground plane employing proximity feeding. In addition, the BW realized is higher. The multi-band antennas with a modified ground plane in [17] mainly emphasize area reduction along with a reduced crosspolarization level at higherorder mode frequencies. Also antennas reported in [17] offer impedance BW of less than 2% in each band. Designs of regular shape MSA using bow-tie ground plane offering 8% BW on a thinner substrate are reported in [18]. In the proposed work, although a similar ground plane profile is used, the present work only focuses on BW improvement using a simpler structure and thus employs thicker substrate and proximity feeding. Using this more than 30% BW increment against that reported in [18] is achieved. The MSAs proposed here on smaller substrate thickness even yield wider BW. The MSAs in [19, 20] employ narrow slots and slotted stub on the ground plane. The realization of these structures is complex due to their small dimensions. The W-shape and U-shape ground planes reported in [21, 22] change the effective height of the substrate due to their protruding structures. But here the planarity of the antenna is lost. Against the proposed configuration on lower substrate thickness, wideband E-shape MSA reported in [28] requires a smaller substrate thickness due to the use of a printed L-C circuit. But in [28], design guidelines for the printed L-C circuit are not given. Also the realized BW is much smaller than that obtained in the proposed designs.

In all the proposed modified ground plane designs, a reduction in the cross-polarization level is observed in the E-plane, over a wide angular range. However, the same is not observed in the H-plane, which is due to the thicker proximity feed. Hence, the present study does not claim to present lower cross-polar design, but the simpler wideband configurations. Thus, simpler wideband configurations of regular shape MSAs offering higher or comparable BW as against the reported slot cut variations is the new technical contribution in the proposed work. With simpler modifications in the ground plane, BW increase of the order of 12–24%, with a smaller reduction in the broadside gain ($\sim$ 1–1.5 dBi) is achieved in the proposed designs. Further, using the proximity feed, modified ground plane profile helps in achieving wider BW (8–20% increase) on smaller substrate thickness (reduction in thickness by 0.02–0.03λ_g) against the original thicker substrate design employing conventional ground plane. In the proposed designs, a study was also carried out with a larger ground plane ($L_g > 15$ cm). It showed similar results for BW enhancement when the slot reached below the patch boundaries. Therefore for maintaining the low profile, ground plane size as mentioned above is selected. Further, the proposed designs are optimized using the parametric process in 1000 MHz frequency band, where they can find applications in GSM and mobile communication systems. The resonant length formulations for patch modes are not presented here since modal frequencies are not affected, but only the quality factor which enhances the MSA BW.

4. CONCLUSIONS

Wideband designs of regular shape MSA using bow-tie and H-shape ground plane profiles are presented. An optimum result in terms of BW and gain together is obtained in SMSA and CMSA designs. Using the bow-tie shape ground, CMSA yields 12% BW improvement whereas SMSA yields 24%. Using the H-shape ground plane, CMSA yields BW increment by 17%. Apart from the BW enhancement, the modified shape of the ground plane helps in optimizing the proximity fed antennas on smaller substrate thickness and offers nearly 8–20% increase in the BW against the conventional ground plane employing thicker substrate. Thus, the proposed designs with simpler ground plane modification offer BW increase by 12–24%, substrate thickness reduction by 0.02–0.03λ_g, the broadside peak gain of above 6 dBi, and with F/B ratio of not more than 8–10 dB over the complete BW.

REFERENCES

1. Kumar, G. and K. P. Ray, *Broadband Microstrip Antennas*, Artech House, 2003.
2. Vandenbosch, G. A. E. and A. R. Van de Capelle, "Study of the capacitively fed microstrip antenna element," *IEEE Transactions on Antennas and Propagation*, Vol. 42, No. 12, 1648–1652, December 1994.
3. Cheng, B., Z. Du, and D. Huang, "A differentially fed broadband multimode microstrip antenna," *IEEE Antennas and Wireless Propagation Letters*, Vol. 19, No. 5, 771–775, March 2020.

4. Yoo, J. U. and H. W. Son, "A simple compact wideband microstrip antenna consisting of three staggered patches," *IEEE Antennas and Wireless Propagation Letters*, Vol. 19, No. 12, 2038–2042, September 2020.
5. Yang, D., H. Zhai, C. Guo, and H. Li, "A compact single-layer wideband microstrip antenna with filtering performance," *IEEE Antennas and Wireless Propagation Letters*, Vol. 19, No. 5, 801–805, March 2020.
6. Radavaram, S. and M. Pour, "Wideband radiation reconfigurable microstrip patch antenna loaded with two inverted U-Slots," *IEEE Transactions on Antennas and Propagation*, Vol. 67, No. 3, 1501–1508, December 2018.
7. Guo, Y. X., K. M. Luk, K. F. Lee, and Y. L. Chow, "Double U-slot rectangular patch antenna," *Electronics Letters*, Vol. 34, No. 19, 1805–1806, September 1998.
8. Zhang, X., K. D. Hong, L. Zhu, X. K. Bi, and T. Yuan, "Wideband differentially-fed patch antennas under dual high-order modes for stable high gain," *IEEE Transactions on Antennas and Propagation* Vol. 69, No. 1, 1–5, July 2020.
9. Tiwari, R. N., P. Singh, and B. K. Kanaujia, "Butter fly shape compact microstrip antenna for wideband applications," *Progress In Electromagnetics Research Letters*, Vol. 69, 45–50, 2017.
10. Wu, Z. F., W. J. Lu, J. Yu, and L. Zhu, "Wideband null frequency scanning circular sector patch antenna under triple resonance," *IEEE Transactions on Antennas and Propagation*, Vol. 68, No. 11, 7266–7274, May 2020.
11. Lu, W. J., Q. Li, S. G. Wang, and L. Zhu, "Design approach to a novel dual-mode wideband circular sector patch antenna," *IEEE Transactions on Antennas and Propagation*, Vol. 65, No. 10, 4980–4990, July 2017.
12. Mandal, K. and P. P. Sarkar, "High gain wide-band U-shaped patch antennas with modified ground planes," *IEEE Transactions on Antennas and Propagation*, Vol. 61, No. 4, 2279–2282, January 2013.
13. Mondal, K. and P. P. Sarkar, "Half hexagonal broadband high gain microstrip patch antenna for mobile and radar applications," *Microwave and Optical Technology Letters*, Vol. 58, No. 5, 1028–1032, May 2016.
14. Mondal, K. and P. P. Sarkar, "M-shaped broadband microstrip patch antenna with modified ground plane," *Microwave and Optical Technology Letters*, Vol. 57, No. 6, 1308–1312, June 2015.
15. Bhatia, S. S., A. Sahni, and S. B. Rana, "A novel design of compact monopole antenna with defected ground plane for wideband applications," *Progress In Electromagnetics Research M*, Vol. 70, 21–31, 2018.
16. *IE3D Software*, Version 12.
17. Kadam, P. A. and A. A. Deshmukh, "Modified ground plane multi-band rectangular microstrip antennas with reduced cross polar radiation," *Progress In Electromagnetics Research C*, Vol. 100, 59–71, 2020.
18. Kadam, P. A. and A. A. Deshmukh, "Designs of regular shape microstrip antennas backed by bow-tie shape ground plane for enhanced antenna characteristics," *AEU-International Journal of Electronics and Communications*, Vol. 137, 1–9, 2021.
19. Jyoti Gogoi, P., D. Jyoti Gogoi, and N. S. Bhattacharyya, "Modified ground plane of patch antenna for broadband applications in C-band," *Microwave and Optical Technology Letters*, Vol. 58, No. 5, 1074–1078, May 2016.
20. Kandwal, A., R. Sharma, and S. K. Kumar, "Bandwidth enhancement using Z-shaped defected ground structure for a microstrip antenna," *Microwave and Optical Technology Letters*, Vol. 55, No. 10, 2251–2254, October 2013.
21. Wong, K. L., C. L. Tang, and J. Y. Chiou, "Broadband probe-fed patch antenna with a W-shaped ground plane," *IEEE Transactions on Antennas and Propagation*, Vol. 50, No. 6, 827–831, August 2002.
22. Hsu, W. H. and K. L. Wong, "Broadband probe-fed patch antenna with a U-shaped ground plane for cross-polarization reduction," *IEEE Transactions on Antennas and Propagation*, Vol. 50, No. 3, 352–355, August 2002.

23. Huang, J., "The finite ground plane effects on the microstrip antenna radiation patterns," *IEEE Transactions on Antennas and Propagation*, Vol. 31, No. 4, 649–653, July 1983.
24. Noghanian, S. and L. Shafai, "Control of microstrip antenna radiation characteristics by ground plane size and shape," *IEE Proceedings Microwave Antennas and Propagation*, Vol. 145, No. 3, 207–212, June 1998.
25. Rajo-Iglesias, E., L. Inclán-Sánchez, and Ó. Quevedo-Teruel, "Back radiation reduction in patch antennas using planar soft surfaces," *Progress In Electromagnetics Research Letters*, Vol. 6, 123–130, 2009.
26. Lee, H. M. and W. S Choi, "Effect of partial ground plane removal on the radiation characteristics of a microstrip antenna," *Wireless Engineering and Technology*, Vol. 4, 5–12, 2013.
27. Alias, H., M. T. Ali, S. Subahir N. Ramli, M. A. Sulaiman, and S. Kayat, "A back lobe reduction of aperture coupled microstrip antenna using DGS," *Proceedings of 10th International Conference on Electrical Engineering/Electronics, Computer, Telecommunications and Information Technology*, Thailand, May 15–17, 2013, DOI: 10.1109/ECTICon.2013.6559514.
28. Chen, Y., S. Yang, and Z. Nie, "Bandwidth enhancement method for low profile E-shaped microstrip patch antennas," *IEEE Transactions on Antennas and Propagation*, Vol. 58, No. 7, 2442–2447, 2010.
29. Oka, N. C. M., T. Uchida, and S. Nitta, "Influence of ground plane width on reduction of radiated emission from printed circuit boards," *Electronics and Communications in Japan, Part 2*, Vol. 84, No. 1, 21–31, 2001.
30. Watanabe, T., O. Wada, T. Miyashita, and R. Koga, "Common mode current generation caused by difference of unbalance of transmission lines on a printed circuit board with narrow ground pattern," *IEICE Trans. Communication*, Vol. E83-B, No. 3, 593–599, March 2000.